

Time-separated entangled light pulses from a single-atom emitter

David Vitali,¹ Priscilla Cañizares,¹ Jürgen Eschner,² and Giovanna Morigi³

¹ *Dipartimento di Fisica, Università di Camerino, 62032 Camerino, Italy,*

² *ICFO - Institut de Ciències Fotoniques, Mediterranean Technology Park, 08860 Castelldefels (Barcelona), Spain*

³ *Departament de Física, Universitat Autònoma de Barcelona, 08193 Bellaterra, Spain*

(Dated: February 23, 2008)

The controlled interaction between a single, trapped, laser-driven atom and the mode of a high-finesse optical cavity allows for the generation of temporally separated, entangled light pulses. Entanglement between the photon-number fluctuations of the pulses is created and mediated via the atomic center-of-mass motion, which is interfaced with light through the mechanical effect of atom-photon interaction. By means of a quantum noise analysis we determine the correlation matrix which characterizes the entanglement, as a function of the system parameters. The scheme is feasible in experimentally accessible parameter regimes. It may be easily extended to the generation of entangled pulses at different frequencies, even at vastly different wavelengths.

PACS numbers: 42.50.Dv, 32.80.Qk, 32.80.Lg

I. INTRODUCTION

The increasing interest in realizing quantum networks by means of atoms and photons has risen the issue of achieving full coherent control on atom-photon interactions. Photonic interfaces with atomic ensemble, namely, with a macroscopic number of atoms, have been explored in several milestone experiments, which demonstrated the generation of single photon sources [1], two-mode squeezing in the polarization of the emitted light [2], atomic memory for quantum states of light [3, 4, 5], entanglement of remote ensembles [6], and teleportation between light and matter [7].

Complementary to this approach, photonic interfaces using single atoms can take advantage of the large level of control that can be achieved on the atomic internal and external degrees of freedom. For instance, in microwave cavity QED quantum state and entanglement engineering using single atoms have been demonstrated [8, 9]. In the optical regime, milestone experiments demonstrated the realization of one-atom laser [10, 11], revealed the mechanical forces of single photons on single atoms [12, 13, 14], achieved the controlled interaction of a trapped ion and a cavity [15, 16], yielding single-photon generation on demand [17, 18, 19], and characterized the entanglement between a single atom and its emitted photon [20, 21]. This latter step was instrumental for establishing entanglement between two distant trapped particles by projective measurement of the emitted photon [22]. Most recently, reversible quantum state transfer between light and atoms in a cavity have been experimentally demonstrated [23]. These results constitute relevant progress towards the realization of quantum networks with single atoms [24, 25].

Possible implementation of quantum networks with continuous variables [26] using single atoms as interfaces requires the controlled interaction of light with the atom external degrees of freedom, which exploits the mechanical effects of light-atom interactions [27, 28, 29]. Using these concepts, in a recent proposal we predicted

that a single atom, confined inside a resonator, can act as a quantum medium, generating quantum correlations in the emitted light [30, 31]. Such correlations can be two-mode squeezing type of correlations, which for bipartite Gaussian systems are synonymous of EPR-entanglement [26, 32]. In particular, under suitable conditions, two classical light (laser) pulses, temporally separated at the input, exhibit two-mode squeezing type of correlations at the output of this kind of device, as sketched in Fig. 1. In this case the quantum state of the atomic motion serves as intermediate memory which mediates the entanglement between the first and second pulse at the cavity output. Variation of the laser parameters, driving the atom, allows for tuning the degree of entanglement between the pulses.

In this work, we analyze the efficiency of the proposal for temporally-separated entangled pulses with single atoms [30, 31] by using a quantum Langevin equation description. This description permits us to determine the correlation matrix and hence the amount of entanglement one obtains using experimentally accessible parameter regimes. We show that this proposal is viable to existing experiments, hence providing an important step towards continuous-variable photonic interfaces with single atoms. We remark that here the atom acts as a source of continuous variable “time-bin” entangled pulses, which could be an alternative solution for secure communication [33] with respect to those employing single-photon qubits [34].

This article is organized as follows. In Sec. II the model determining the system’s dynamics is introduced, and the quantum Langevin Equations for the coupled dynamics between atomic motion and cavity mode are derived. In Sec. III the corresponding correlation matrix for the two propagating correlated pulses is determined and the degree of entanglement characterized. In Sec IV entanglement is discussed as a function of the experimental parameters. The conclusions and outlooks are presented

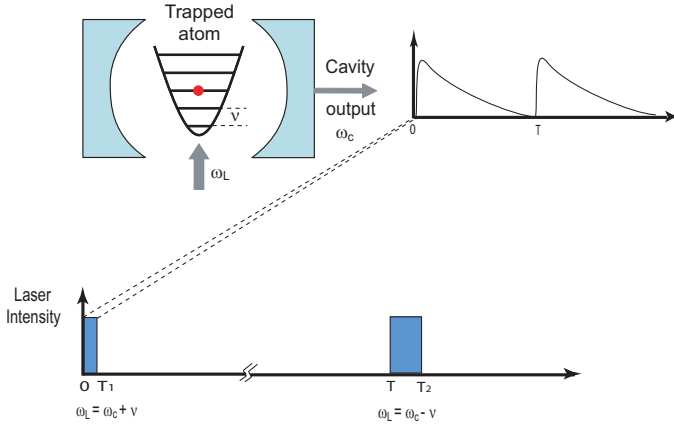


FIG. 1: A trapped atom is confined by a harmonic potential of frequency ν inside a resonator. The atomic dipole is driven by two temporally separated laser pulses, whose intensity as a function of time is displayed at the bottom, and couple with a cavity mode at frequency ω_c . The intensities of the two emitted pulses at the cavity output are shown as a function of time. In this article we show that, in a suitable parameter regime, they exhibit quadrature entanglement.

in Sec. V, and the appendices report the details of the derivations in Sec. II and Sec. III.

II. THEORETICAL DESCRIPTION

We summarize the basic concepts at the basis of the proposal for the creation of pairs of temporally separated, continuous-variable (CV) entangled pulses. Let us consider a single atom in a harmonic trap of frequency ν and confined inside a resonator, in the setup sketched in Fig. 1. Be b, b^\dagger the annihilation and creation operator of an excitation of the quantized motion inside the trap. The atomic dipole couples with a cavity mode at frequency ω_c , which is far-off resonance from the dipole frequency ω_0 . We denote by a, a^\dagger the annihilation and creation operator of a cavity photon. A first laser pulse at frequency $\omega_L \simeq \omega_c + \nu$ illuminates the atom in the time interval $[0, T_1]$. In this regime, the simultaneous emission of a cavity photon and of a vibrational quantum of the atom is resonantly enhanced, see Fig. 2(a), and the relevant dynamics are described the effective Hamiltonian

$$H^{(1)} = i\hbar\chi_1 a^\dagger b^\dagger + \text{H.c.}, \quad (1)$$

where χ_1 is the transition amplitude of the resonant process. This Hamiltonian describes an interaction giving rise to two-mode squeezing, i.e., CV entanglement between the center-of-mass oscillator and the cavity mode. If the pulse is implemented for a sufficiently short time, so that photon leakage out of the cavity has negligible effects and the dynamics can be assumed to be coherent,

at the end of the pulse the cavity mode and the atom's vibrational motion will be entangled. Cavity decay will give rise to a propagating pulse, whose photon number is quantum-correlated with the vibrational phonon number [28, 29].

We then assume that at a time $T > T_1$ a second laser pulse tuned to the frequency $\omega_L \simeq \omega_c - \nu$ drives the atom till the time T_2 . In this regime, one has resonant enhancement of the emission of a cavity photon with the simultaneous *absorption* of a vibrational quantum, see Fig. 2(b). The effective dynamics is described by the Hamiltonian

$$H^{(2)} = i\hbar\chi_2 a^\dagger b + \text{H.c.}, \quad (2)$$

where χ_2 is the transition amplitude of the resonant process. Again, we assume that cavity decay can be safely neglected, so that the dynamics is coherent. When the pulse duration $\delta T = T_2 - T$ is appropriately chosen, the quantum state of the center-of-mass motion at time T is completely transferred to the cavity mode at time T_2 . Consequently, by cavity decay a second pulse at the cavity output will be generated, which is entangled with the first one [30, 31].

This proposal is based on the assumption that during the laser pulses the dynamics is essentially described by the effective Hamiltonian (1) and (2), while detrimental effects like atomic spontaneous emission, vacuum optical input noise entering the cavity, and fluctuations of the trapping potential can be neglected. These assumptions are justified in certain parameter regimes, which have been discussed in [30, 31]. The scope of this work is to explore the robustness of the scheme when detrimental effects are small but cannot be *a priori* neglected in the dynamical equations. At this purpose, in this section we adopt a quantum Langevin equations treatment, taking into account all sources of noise. This permits us to determine the correlation matrix for the generated pulses, which are discussed in Sec. III, and to quantify their degree of entanglement for a wide range experimental parameters, as shown in Sec IV.

A. The system

We consider an atom of mass m , whose center-of-mass motion takes place essentially in one-dimension. We assume, in fact, that the radial potential is sufficiently steep, so that the radial motion can be considered frozen out. Be the motion along the \hat{x} -axis, and be x, p the position and momentum of the atomic center of mass. The center of mass is a harmonic oscillator with angular frequency ν , whose Hamiltonian reads

$$H_{\text{mec}} = \hbar\nu \left(b^\dagger b + \frac{1}{2} \right), \quad (3)$$

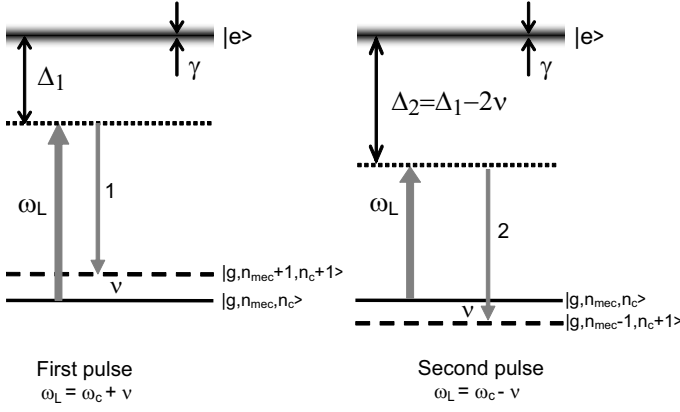


FIG. 2: Relevant energy level and resonant transitions during the two pulses. Here, $|g\rangle$ and $|e\rangle$ denote ground and excited state of the atomic dipole transition with linewidth γ , $|n_c\rangle$ the number of cavity photons, and $|n_{mec}\rangle$ the number of vibrational excitations. (a) First pulse: The laser is detuned by Δ_1 from the dipole, and by $\delta_1 = \nu$ from the cavity mode, driving resonantly the two-photon transition $|g, n_{mec}, n_c\rangle \rightarrow |g, n_{mec} + 1, n_c + 1\rangle$. These processes generate two-mode squeezing between cavity and motion. (b) Second pulse: The laser is detuned by $\Delta_2 = \Delta_1 - 2\nu$ from the dipole, hence driving resonantly the two-photon transition $|g, n_{mec}, n_c\rangle \rightarrow |g, n_{mec} - 1, n_c + 1\rangle$. Choosing the pulse duration properly, quantum-state transfer between motion and cavity mode can be achieved, see [27, 28]. Note that by varying the frequency of the second laser pulse and/or the atomic transition which it excites, the two output pulses can be at different frequencies or wavelengths.

where x, p are related to the annihilation and creation operators b and b^\dagger of a quantum of vibrational energy $\hbar\nu$ by the relations $x = \sqrt{\hbar/2m\nu}(b + b^\dagger)$ and $p = i\sqrt{\hbar m\nu/2}(b^\dagger - b)$. The relevant atomic internal degrees of freedom are the ground state $|g\rangle$ and the excited state $|e\rangle$, which form a dipole transition with moment \mathbf{d} and frequency ω_0 . The transition couples to one optical mode of the cavity at frequency ω_c and to the laser, a classical field, which is a pulsed excitation whose central frequency ω_L is tuned from a pulse to the next. We define our model in the reference frame rotating at ω_L , remembering that the frequency changes from the first to the second pulse, and the two reference frames are hence related by a global time-dependent phase. In the reference frame rotating at ω_L the total Hamiltonian is $H = H_a + H_c + H_{int}$. Here,

$$H_a = -\hbar\Delta|e\rangle\langle e| + H_{mec} \quad (4)$$

is the atomic Hamiltonian with $\Delta = \omega_L - \omega_0$, while

$$H_c = -\hbar\delta a^\dagger a \quad (5)$$

describes the dynamics of the cavity mode, with $\delta = \omega_L - \omega_c$. The coupling between atom and fields is described by

$$H_{int} = \hbar(\sigma^\dagger B(t) + \sigma B^\dagger(t)) \quad (6)$$

where $\sigma = |g\rangle\langle e|$ and $\sigma^\dagger = |e\rangle\langle g|$ denote the dipole lowering and raising operators and $B(t)$ is the operator for the field degrees of freedom, which we decompose into laser and cavity components, $B(t) = B_L(t) + B_c$. The cavity term is $B_c = g_c \cos(kx \cos \theta_c + \phi_c)a$, where g_c is the coupling strength and the cavity mode wave vector \vec{k} ($k = |\vec{k}|$) forms an angle θ_c with the axis \hat{x} of the motion. The angle ϕ_c takes into account the position of the trap center inside the cavity. From now on we will assume that the atomic motion is in the Lamb-Dicke regime, such that the atom-photon interactions can be expanded at second order in the Lamb-Dicke parameter $\eta = k\sqrt{\hbar/2m\nu}$. In this limit term B_c takes the form [35]

$$B_c = g_c \cos \phi_c a \left(1 - \frac{\eta^2}{2} \cos^2 \theta_c (2b^\dagger b + 1) \right) - \eta \cos \theta_c g_c \sin \phi_c a (b^\dagger + b). \quad (7)$$

The laser term is $B_L(t) = \Omega(t)e^{ikx \cos \theta_L}$, where $\Omega(t)$ is the (slowly-varying) Rabi frequency and θ_L is the angle between the direction of propagation of the laser and the trap axis. In the Lamb-Dicke regime this operator reads

$$B_L(t) = \Omega(t) \left(1 - \frac{\eta^2}{2} \cos^2 \theta_L (2b^\dagger b + 1) \right) + i\eta\Omega(t) \cos \theta_L (b^\dagger + b). \quad (8)$$

B. Quantum Langevin equations

The full dynamics of the system must take into account the coupling with the environment, which is here represented by the dipole fluctuations, giving rise to spontaneous emission, by vacuum fluctuations at the cavity input, giving rise to cavity decay, and by fluctuations of the trapping potentials, which are responsible of damping and loss of quantum coherence of the center-of-mass motion. Cavity decay is described by the Markovian noise operator $a^{in}(t)$, while the heating due to the fluctuations of the trap potential is described by the phenomenological Markovian input noise operator $b^{in}(t)$ acting on the atomic motion. These two noise sources are mutually uncorrelated and have zero mean value, and their only nonzero second-order correlation functions are

$$\langle a^{in}(t)a^{in}(t')^\dagger \rangle = \delta(t - t'), \quad (9)$$

$$\langle b^{in}(t)b^{in}(t')^\dagger \rangle = (\bar{N} + 1)\delta(t - t'), \quad (10)$$

$$\langle b^{in}(t)^\dagger b^{in}(t') \rangle = \bar{N}\delta(t - t'), \quad (11)$$

where \bar{N} is mean thermal vibrational number of the effective thermal reservoir coupling to the atom center-of-mass motion. We denote by κ_b the damping rate of the vibrational motion. Pure heating corresponds to the limit of $\kappa_b \rightarrow 0$, simultaneously with an infinite temperature of the associated effective reservoir, i.e., $\bar{N} \rightarrow \infty$, with $2\kappa_b\bar{N} \equiv \kappa_h$, the heating rate, kept constant [37].

The input noise terms associated with spontaneous emission are more involved because the latter affects both

the internal and the motional degree of freedom of the atom, due to the presence of recoil. This effect has been neglected in the analysis presented in [38], which focussed on the c.w.-generation of entangled light, and will be systematically taken into account in this work. At this purpose, the corresponding Langevin force must be defined. At second order in the Lamb-Dicke parameter η , the Langevin force operator $F(t)$ associated with spontaneous emission is given by (see also its detailed derivation in App. A)

$$F(t) = \sqrt{\gamma} \int d\cos\theta \sqrt{\mathcal{N}(\cos\theta)} f_{\theta}^{in}(t) \times \left(1 - \frac{\eta^2}{2} \cos^2\theta (2b^{\dagger}b + 1) + i\eta \cos\theta (b^{\dagger} + b) \right), \quad (12)$$

where γ is the spontaneous emission rate of level $|e\rangle$, and $\mathcal{N}(\cos\theta)$ is the dipole pattern of emission, such that $\int d\cos\theta \mathcal{N}(\cos\theta) = 1$. The integral is over the angle θ between the wave vector of the emitted photon and the axis of the motion, and $f_{\theta}^{in}(t)$ are the zero-mean, angle-dependent Langevin forces, with the only nonzero correlation function

$$\langle f_{\theta}^{in}(t) f_{\theta'}^{in\dagger}(t') \rangle = \delta(\theta - \theta') \delta(t - t'). \quad (13)$$

It is convenient to isolate the zeroth-order term in the Lamb-Dicke parameter in Eq. (12) and to rewrite $F(t)$ as

$$F(t) = f^{in}(t) + F_{nl}(t), \quad (14)$$

with the zeroth-order term

$$f^{in}(t) = \int d\cos\theta \sqrt{\mathcal{N}(\cos\theta)} f_{\theta}^{in}(t) \quad (15)$$

possessing the correlation function

$$\langle f^{in}(t) f^{in\dagger}(t') \rangle = \delta(t - t'). \quad (16)$$

Term $F_{nl}(t) = F(t) - f^{in}(t)$ is hence at higher order in η . We shall see that spontaneous emission noise is

essentially described by $f^{in}(t)$, because the higher order term $F_{nl}(t)$ gives a negligible contribution to the Langevin equations in the parameter regime considered in this work (see App. B).

In the frame rotating at the laser frequency the quantum Heisenberg–Langevin equations (HLE) of the system read [36]

$$\dot{a}(t) = (i\delta - \kappa)a(t) + i\sigma(t) [B^{\dagger}(t), a(t)] + \sqrt{2\kappa}a^{in}(t) \quad (17)$$

$$\dot{b}(t) = -i\nu b(t) + i\sigma(t) [B^{\dagger}(t) + F^{\dagger}(t), b(t)] + i\sigma(t)^{\dagger} [B(t) + F(t), b(t)] - \kappa_b b(t) + \sqrt{2\kappa_b}b^{in}(t), \quad (18)$$

$$\dot{\sigma}(t) = \left[i\Delta - \frac{\gamma}{2} \right] \sigma(t) + i\sigma_z(t) (B(t) + F(t)), \quad (19)$$

$$\dot{\sigma}_z(t) = 2i\sigma(t) [B^{\dagger}(t) + F^{\dagger}(t)] - 2i\sigma^{\dagger}(t) [B(t) + F(t)] - \gamma(\sigma_z(t) + 1)/2, \quad (20)$$

where $\sigma_z = \sigma^{\dagger}\sigma - \sigma\sigma^{\dagger}$ and κ is the decay rate of the cavity mode.

In the cases we are going to consider both laser as well as cavity mode are tuned far-off resonance from the dipole transition, i.e., $|\Delta| \gg \Omega, g, |\delta|, \gamma$. In this regime the atomic internal degrees of freedom can be eliminated in second order perturbation theory. Hence, we neglect the time evolution of σ_z , Eq. (20), and approximate $\sigma_z(t) \approx -1$. Correspondingly, Eq. (19) becomes

$$\dot{\sigma}(t) = -\left(\frac{\gamma}{2} - i\Delta \right) \sigma(t) - iB(t) - iF(t), \quad (21)$$

whose formal solution is

$$\sigma(t) = e^{-(\frac{\gamma}{2} - i\Delta)t} \sigma(0) - i \int_0^t ds e^{-(\frac{\gamma}{2} - i\Delta)s} [B(t-s) + F(t-s)]. \quad (22)$$

We insert solution (22) into the other HLE and neglect the transient term as we are interested in the dynamics at times which are much larger than $1/|\Delta|$. The resulting HLE for cavity and trap oscillators are

$$\dot{a}^{\dagger}(t) = -i\delta a^{\dagger}(t) - \int_0^t ds e^{-(\frac{\gamma}{2} + i\Delta)s} [B^{\dagger}(t-s) + F^{\dagger}(t-s)] [B(t), a^{\dagger}(t)] - \kappa a^{\dagger}(t) + \sqrt{2\kappa}a^{in\dagger}(t), \quad (23)$$

$$\begin{aligned} \dot{b}(t) = & -i\nu b(t) + \int_0^t ds e^{-(\frac{\gamma}{2} - i\Delta)s} [B(t-s) + F(t-s)] [B^{\dagger}(t) + F^{\dagger}(t), b(t)] \\ & - \int_0^t ds e^{-(\frac{\gamma}{2} + i\Delta)s} [B^{\dagger}(t-s) + F^{\dagger}(t-s)] [B(t) + F(t), b(t)] - \kappa_b b(t) + \sqrt{2\kappa_b}b^{in}(t), \end{aligned} \quad (24)$$

where we have not taken care of operator ordering, since, as we shall see, within the validity limit of our treatment

these integral terms will generate only linear contributions. We now determine the solutions of these equa-

tions for the dynamics during the first pulse, between the pulses, and during the second pulse.

1. Dynamics during the first laser pulse

We first consider the dynamics during the first pulse, i.e., in the time interval $0 \leq t \leq T_1$, where we assume a square laser pulse with central angular frequency ω_{L1} and constant Rabi frequency $\Omega(t) = \Omega_1$ during this time interval. Correspondingly, we denote by $\Delta = \Delta_1$ and $\delta = \delta_1$ the detuning of the laser from the atomic and cavity frequency. We assume that the laser is far-off resonance from the atomic transition, i.e., Δ_1 is negative and $|\Delta_1| \gg \Omega_1, g, \gamma$. The laser frequency is tuned to the value $\omega_{L1} \simeq \omega_c + \nu$, namely, the cavity mode is resonant with the Stokes motional sideband of the laser light. This condition allows to establish a parametric-amplifier type of interaction between cavity mode and motion, which is selectively enhanced provided that the Stokes sideband is spectrally resolved, namely, when $\nu T_1 \gg 1$ and $\nu \gg \kappa, \kappa_b$. In particular, we take into account the presence of a.c.-Stark shifts $\delta\nu$, due to the mechanical coupling with laser and cavity modes, by tuning the laser

frequency to the value

$$\omega_{L1} = \omega_c + \nu', \quad (25)$$

and hence $\delta'_1 = \nu'$, with $\nu' = \nu + \delta\nu$ and $\delta'_1 = \delta_1 - \delta'$, and δ' accounts for possible a.c.-Stark shifts due to off-resonant couplings. The value of $\delta\nu$ is determined in a self-consistent way, which is extensively discussed in App. B, see also [38].

Starting from Eqs. (23)-(24), in this parameter regime we derive the effective HLE, which describe the coherent interaction between the cavity mode and the vibrational motion during the first laser pulse, in the presence of losses and noise processes due to spontaneous emission, cavity decay, and vibrational heating. For later convenience, we study the equations in the reference frame rotating at the cavity-mode frequency, which is obtained from the reference frame of the laser frequency by the transformation

$$\tilde{a}^\dagger(t) = e^{i\nu't} a^\dagger(t), \quad (26)$$

$$\tilde{b}(t) = e^{i\nu't} b(t). \quad (27)$$

In this reference frame, the HLE read

$$\dot{\tilde{a}}^\dagger(t) = \chi_1^* \tilde{b}(t) - (\kappa + \kappa_L) \tilde{a}^\dagger(t) + \sqrt{2\kappa} \tilde{a}^{in\dagger}(t) + \sqrt{2\kappa_L} \tilde{a}_-^{in\dagger}(t), \quad (28)$$

$$\dot{\tilde{b}}(t) = \chi_1 \tilde{a}^\dagger(t) - (\kappa_b + \kappa_{+1}^b - \kappa_{-1}^b) \tilde{b}(t) + \sqrt{2\kappa_b} \tilde{b}^{in}(t) + \sqrt{2\kappa_{+1}^b} \tilde{a}_+^{in}(t) - \sqrt{2\kappa_{-1}^b} \tilde{a}_-^{in\dagger}(t). \quad (29)$$

The equations are at second order in the Lamb-Dicke parameter, and have been obtained neglecting off-resonant terms. The steps of the derivation are reported in App. B.

We now define and discuss each term appearing in the equations. The effective coupling between motion and cavity mode is

$$\chi_1 = \eta \frac{\Omega_1 g_c^* \cos \phi_c}{\Delta_1} (\cos \theta_L + i \tan \phi_c \cos \theta_c), \quad (30)$$

and corresponds to the Raman processes in which laser photons are scattered into the cavity mode with a change in the center-of-mass excitation. The new noise operators appearing in Eqs. (28)-(29), $\tilde{a}_\pm^{in}(t)$, are defined as

$$\tilde{a}_-^{in}(t) = f^{in}(t) e^{-i\nu't}, \quad (31)$$

$$\tilde{a}_+^{in}(t) = f^{in}(t) e^{i\nu't}, \quad (32)$$

and describe the coupling with external optical modes due to the photons scattered by the atom. They possess the same correlation functions of the spontaneous emission noise $f^{in}(t)$, and at the time scales of interest, $\nu't \gg 1$, they are uncorrelated from each other. These noise components affect both the cavity mode and the vibrational motion. In particular, $\tilde{a}_-^{in}(t)$ describes quantum noise associated with incoherent scattering by the atom of a cavity photon into the external modes at rate

$$\kappa_L = \frac{\gamma}{2} \frac{|g_c|^2 \cos^2 \phi_c}{\gamma^2/4 + (\Delta_1 - \nu')^2}, \quad (33)$$

while the corresponding input noise scales with

$$\bar{\kappa}_L = -\sqrt{\frac{\gamma}{2}} \frac{g_c \cos \phi_c}{\gamma/2 + i(\Delta_1 - \nu')}, \quad (34)$$

where $\kappa_L = |\bar{\kappa}_L|^2$. The two noise terms in Eqs. (31)-(32) also affect the atom's motion due to the mechanical effects of the scattering of laser photons. The incoherent change of vibrational quanta due to scattering of laser photons takes place at rates [39]

$$\kappa_{\pm 1}^b = \eta^2 \frac{\gamma}{2} \frac{|\Omega_1|^2 \cos^2 \theta_L}{\gamma^2/4 + (\Delta_1 \pm \nu')^2}, \quad (35)$$

while the corresponding terms $\bar{\kappa}_{\pm 1}^b$ scaling the input noise are given by (see App. B)

$$\bar{\kappa}_{\pm 1}^b = \pm i \eta \sqrt{\frac{\gamma}{2}} \frac{\Omega_1 \cos \theta_L}{\gamma/2 \mp i(\Delta_1 \pm \nu')}, \quad (36)$$

so that $\kappa_{\pm 1}^b = |\bar{\kappa}_{\pm 1}^b|^2$. The formal solution of Eqs. (28)-(29) at time $t = T_1$ reads

$$\begin{aligned}\tilde{a}^\dagger(T_1) &= g_{-1}(T_1)\tilde{a}^\dagger(0) + \chi_1^* f_1(T_1)\tilde{b}(0) + \chi_1^* \int_0^{T_1} ds f_1(T_1 - s) \left[\sqrt{2\kappa_b}\tilde{b}^{in}(s) + \sqrt{2\kappa_{+1}^b}\tilde{a}_+^{in}(s) - \sqrt{2\kappa_{-1}^b}\tilde{a}_-^{in\dagger}(s) \right] \\ &\quad + \int_0^{T_1} ds g_{-1}(T_1 - s) \left[\sqrt{2\kappa}\tilde{a}^{in\dagger}(s) + \sqrt{2\kappa_L}\tilde{a}_-^{in\dagger}(s) \right],\end{aligned}\quad (37)$$

$$\begin{aligned}\tilde{b}(T_1) &= \chi_1 f_1(T_1)\tilde{a}^\dagger(0) + g_{+1}(T_1)\tilde{b}(0) + \int_0^{T_1} ds g_{+1}(T_1 - s) \left[\sqrt{2\kappa_b}\tilde{b}^{in}(s) + \sqrt{2\kappa_{+1}^b}\tilde{a}_+^{in}(s) - \sqrt{2\kappa_{-1}^b}\tilde{a}_-^{in\dagger}(s) \right] \\ &\quad + \chi_1 \int_0^{T_1} ds f_1(T_1 - s) \left[\sqrt{2\kappa}\tilde{a}^{in\dagger}(s) + \sqrt{2\kappa_L}\tilde{a}_-^{in\dagger}(s) \right],\end{aligned}\quad (38)$$

where we have introduced the time-dependent functions

$$g_{\pm 1}(t) = e^{-\kappa_1 s t} \left[\cosh(\theta_1 t) \pm \frac{\kappa_{1D}}{\theta_1} \sinh(\theta_1 t) \right], \quad (39)$$

$$f_1(t) = e^{-\kappa_1 s t} \frac{1}{\theta_1} \sinh(\theta_1 t), \quad (40)$$

and the parameters

$$\kappa_{1S} = \frac{\kappa + \kappa_L + \kappa_b + \kappa_{+1}^b - \kappa_{-1}^b}{2}, \quad (41)$$

$$\kappa_{1D} = \frac{\kappa + \kappa_L - \kappa_b - \kappa_{+1}^b + \kappa_{-1}^b}{2}, \quad (42)$$

$$\theta_1 = \sqrt{|\chi_1|^2 + \kappa_{1D}^2}. \quad (43)$$

Equations (37)-(38) describe the dynamics of the coupled motion and cavity mode during the first pulse in presence of quantum noise. By setting all noise terms to zero, $\kappa, \kappa_j = 0$, they reproduce the well-known coherent two-mode squeezing dynamics [36], where entanglement monotonically increases as a function of the interaction time T_1 . The presence of quantum noise sets a limit to the establishing of these dynamics.

2. Dynamics between the two laser pulses

In the time interval $T_1 \leq t \leq T$ the laser is turned off and consequently there are no resonant photon scat-

tering processes which couple the cavity mode and the atom's vibrational motion. The HLE describing the system without laser excitation can be obtained immediately from Eqs. (28)-(29) by setting $\Omega_1 = 0$ and thus $\chi_1 = \kappa_{+1}^b = \kappa_{-1}^b = 0$. The resulting HLE are given by

$$\dot{\tilde{a}}(t) = -(\kappa + \kappa_L) \tilde{a}(t) + \sqrt{2\kappa}\tilde{a}^{in}(t) + \sqrt{2\kappa_L}\tilde{a}_-^{in}(t), \quad (44)$$

$$\dot{\tilde{b}}(t) = i\delta_1^b \tilde{b}(t) - \kappa_b \tilde{b}(t) + \sqrt{2\kappa_b}\tilde{b}^{in}(t), \quad (45)$$

where off-resonant coupling between motion and cavity mode is neglected, and δ_1^b is defined in App. B. This latter term is due to the definition of the reference frame rotating at frequency ν' , which compensates the laser-induced a.c.-Stark shift on the motion: In absence of the laser, this component of the frequency ν' is unbalanced. The assumption of neglecting off-resonant coupling between motion and cavity mode is justified when the cavity-mode wavevector is orthogonal to the axis of the motion, and thus there is no mechanical coupling. In general, it is valid at zero order in the expansion in the small parameter $\eta g \cos \theta_c / |\omega_c - \omega_0|$, which hence imposes a condition on the integration time T under which Eqs. (44)-(45) are valid. The solutions of Eqs. (44)-(45) are

$$\tilde{a}(T) = e^{-(\kappa + \kappa_L)(T - T_1)} \tilde{a}(T_1) + \int_{T_1}^T ds e^{-(\kappa + \kappa_L)(T - s)} \left[\sqrt{2\kappa}\tilde{a}^{in}(s) + \sqrt{2\kappa_L}\tilde{a}_-^{in}(s) \right], \quad (46)$$

$$\tilde{b}(T) = e^{(i\delta_1^b - \kappa_b)(T - T_1)} \tilde{b}(T_1) + \sqrt{2\kappa_b} \int_{T_1}^T ds e^{(i\delta_1^b - \kappa_b)(T - s)} \tilde{b}^{in}(s), \quad (47)$$

where $\tilde{a}(T_1)$ and $\tilde{b}(T_1)$ are given by Eqs. (37)-(38). They yield the observables of interest at time T , before the

second laser pulse is switched on.

3. Dynamics during the second laser pulse

We now consider that in the time interval $T \leq t \leq T_2$ a square pulse of constant Rabi frequency $\Omega(t) = \Omega_2$ and central angular frequency ω_{L2} illuminates the atom. We denote by $\delta_2 = \omega_{L2} - \omega_c$, and $\Delta_2 = \omega_{L2} - \omega_0$ the detuning of the laser frequency from cavity mode and dipole transition, respectively. In the limit in which processes

where absorption of a laser photon and of a phonon is resonant with emission of a cavity photon, $\omega_{L2} \approx \omega_c - \nu$, we derive the HLE from Eqs. (17)-(20), describing the interaction between the cavity mode and the vibrational motion during the second laser pulse, in the presence of losses and noise processes due to spontaneous emission, cavity decay, and vibrational heating,

$$\dot{\tilde{a}}(t) = \chi_2 \tilde{b}(t) - (\kappa + \kappa_L) \tilde{a}(t) + \sqrt{2\kappa} \tilde{a}^{in}(t) + \sqrt{2\kappa_L^*} \tilde{a}_+^{in}(t), \quad (48)$$

$$\dot{\tilde{b}}(t) = -\chi_2^* \tilde{a}(t) - (\kappa_b + \kappa_{+2}^b - \kappa_{-2}^b) \tilde{b}(t) + \sqrt{2\kappa_b} \tilde{b}^{in}(t) + \sqrt{2\kappa_{+2}^b} \tilde{a}_+^{in}(t) - \sqrt{2\kappa_{-2}^b} \tilde{a}_-^{in\dagger}(t), \quad (49)$$

where parameters χ_2 and $\kappa_{\pm 2}^b$ are found from χ_1 and $\kappa_{\pm 1}^b$ by replacing $\Omega_1 \rightarrow \Omega_2$, $\delta_1 \rightarrow \delta_2$, and $\Delta_1 \rightarrow \Delta_2$ in Eqs. (30) and (33). The details of the derivation are

reported in App. B.

The solutions of Eqs. (48)-(49) at the end of the second pulse, $t = T_2$, read

$$\begin{aligned} \tilde{a}(T_2) &= g_{-2}(T_2 - T) \tilde{a}(T) + \chi_2 f_2(T_2 - T) \tilde{b}(T) + \chi_2 \int_T^{T_2} ds f_2(T_2 - s) \left[\sqrt{2\kappa_b} \tilde{b}^{in}(s) + \sqrt{2\kappa_{+2}^b} \tilde{a}_+^{in}(s) - \sqrt{2\kappa_{-2}^b} \tilde{a}_-^{in\dagger}(s) \right] \\ &\quad + \int_T^{T_2} ds g_{-2}(T_2 - s) \left[\sqrt{2\kappa} \tilde{a}^{in}(s) + \sqrt{2\kappa_L^*} \tilde{a}_+^{in}(s) \right], \end{aligned} \quad (50)$$

$$\begin{aligned} \tilde{b}(T_2) &= -\chi_2^* f_2(T_2 - T) \tilde{a}(T) + g_{+2}(T_2 - T) \tilde{b}(T) + \int_T^{T_2} ds g_{+2}(T_2 - s) \left[\sqrt{2\kappa_b} \tilde{b}^{in}(s) + \sqrt{2\kappa_{+2}^b} \tilde{a}_+^{in}(s) - \sqrt{2\kappa_{-2}^b} \tilde{a}_-^{in\dagger}(s) \right] \\ &\quad - \chi_2^* \int_T^{T_2} ds f_2(T_2 - s) \left[\sqrt{2\kappa} \tilde{a}^{in}(s) + \sqrt{2\kappa_L^*} \tilde{a}_+^{in}(s) \right], \end{aligned} \quad (51)$$

where we have introduced

$$g_{\pm 2}(t) = e^{-\kappa_2 s t} \left[\cos(\theta_2 t) \pm \frac{\kappa_{2D}}{\theta_2} \sin(\theta_2 t) \right], \quad (52)$$

$$f_2(t) = e^{-\kappa_2 s t} \frac{1}{\theta_2} \sin(\theta_2 t), \quad (53)$$

and

$$\kappa_{2S} = \frac{\kappa + \kappa_L + \kappa_b + \kappa_{+2}^b - \kappa_{-2}^b}{2}, \quad (54)$$

$$\kappa_{2D} = \frac{\kappa + \kappa_L - \kappa_b - \kappa_{+2}^b + \kappa_{-2}^b}{2}, \quad (55)$$

$$\theta_2 = \sqrt{|\chi_2|^2 - \kappa_{2D}^2}. \quad (56)$$

Equations (50)-(51) give the cavity mode and motion at the end of the second pulse. Setting all decay and noise sources to zero, we recover the ideal polariton dynamics during the second pulse, namely a periodic dynamics at frequency $|\chi_2|$. Ideally, then, the states of the motion and of the cavity mode are swapped when

$T_2 - T = \delta T_2^0$, such that $|\chi_2| \delta T_2^0 = (2\ell + 1)\pi/2$, with ℓ integer number. At these values the function f_2 reaches its maximum, $f_2(\delta T_2^0)|_{\kappa:j=0} = 1$, while g_{-2} vanishes, $g_{-2}(\delta T_2^0)|_{\kappa:j=0} = 0$. The effect of decay and noise is to damp the oscillators, hence to modify the oscillation frequency and the behaviour of functions f_2 , g_{-2} . In particular, the maximum value of $f_2(t)$ is always smaller than unity, and the maxima of f_2 do not occur at the same instants of time in which $g_{-2}(t)$ vanishes. We optimize the process by setting $T_2 - T$ such that it fulfills the condition $g_{-2}(T_2 - T) = 0$. Denoting by $\delta T_2^{opt} = T_2 - T$ the time interval fulfilling this condition, it satisfies the relation

$$\delta T_2^{opt} \equiv \frac{1}{\theta_2} \arctan \frac{\theta_2}{\kappa_{2D}}. \quad (57)$$

III. QUANTIFYING THE ENTANGLEMENT BETWEEN THE TWO PULSES

The two time-separated pulses at the cavity output can be considered as two independent modes, even if they originate from the same intracavity field at different times. In fact, the output field $a^{out}(t)$ is related to the intracavity field $\tilde{a}(t)$ by the input-output relation [36]

$$\tilde{a}^{out}(t) = \sqrt{2\kappa}\tilde{a}(t) - \tilde{a}^{in}(t) \quad (58)$$

and it is characterized by the commutation relation $[\tilde{a}^{out}(t), \tilde{a}^{out\dagger}(t')] = \delta(t - t')$. In order to have a quantity directly related to the detected field, we define the following integrated output field over a generic measurement time T_m [40],

$$\tilde{a}_I^{out}(t, T_m) = \frac{1}{\sqrt{T_m}} \int_t^{t+T_m} dt' \tilde{a}^{out}(t'). \quad (59)$$

The field operators $\tilde{a}_I^{out}(t, T_m)$, form a class of dimensionless bosonic operators, $[\tilde{a}_I^{out}(t, T_m), \tilde{a}_I^{out\dagger}(t, T_m)] = 1$, and they commute, i.e., they describe independent modes, as soon as they do not temporally overlap, that

is, $[\tilde{a}_I^{out}(t, T_m), \tilde{a}_I^{out\dagger}(t', T_m)] = 0$ whenever $|t - t'| > T_m$. The two output pulses we are interested in are therefore those associated with the operators $\tilde{a}_I^{out}(T_1, T_m)$ and $\tilde{a}_I^{out}(T_2, T_m)$. In the present scheme the two pulses are temporally separated and therefore it is natural to consider $T_m < T - T_1$, which automatically warrants the independence of the two integrated output modes.

In order to characterize the entanglement between the two pulses, one usually considers the amplitude and phase quadratures of the two independent modes, which are in this case

$$X^{out}(T_j, T_m) = \frac{\tilde{a}_I^{out}(T_j, T_m) + \tilde{a}_I^{out\dagger}(T_j, T_m)}{\sqrt{2}}, \quad (60)$$

$$P^{out}(T_j, T_m) = \frac{\tilde{a}_I^{out}(T_j, T_m) - \tilde{a}_I^{out\dagger}(T_j, T_m)}{i\sqrt{2}}, \quad (61)$$

and construct the correlation matrix

$$V_{kl}^{out} = \frac{\langle \xi_k^{out} \xi_l^{out} + \xi_l^{out} \xi_k^{out} \rangle}{2}, \quad (62)$$

where we have defined the four-dimensional vector

$$\xi^{out, T} = \{X^{out}(T_1, T_m), P^{out}(T_1, T_m), X^{out}(T_2, T_m), P^{out}(T_2, T_m)\}.$$

In Eq. (62) the averaging corresponds to taking expectation values with respect to the initial state of the system and the environment. We now proceed in determining its elements.

We use the definition in Eq. (59), the input-output relation of Eq. (58), and the explicit solution for $\tilde{a}(t)$ in the two relevant time intervals, $T_j \leq t \leq T_j + T_m$, $j = 1, 2$, which is given by Eq. (46), and get the following expression of the integrated output fields as a function of the intracavity fields at the end of the pulses $\tilde{a}(T_j)$ and

of the input noises:

$$a_I^{out}(T_j, T_m) = \alpha(T_m)\tilde{a}(T_j) + n^{in}(T_j, T_m), \quad (63)$$

with the factor

$$\alpha(T_m) = \sqrt{\frac{2\kappa}{T_m}} \frac{[1 - e^{-(\kappa + \kappa_L)T_m}]}{\kappa + \kappa_L}, \quad (64)$$

and the input noise term

$$\begin{aligned} n^{in}(T_j, T_m) = & \int_{T_j}^{T_j+T_m} dt \frac{\tilde{a}^{in}(t)}{\sqrt{T_m}} \left[\frac{\kappa - \kappa_L}{\kappa + \kappa_L} - \frac{2\kappa}{\kappa + \kappa_L} e^{-(\kappa + \kappa_L)(T_j + T_m - t)} \right] \\ & + \bar{\kappa}_L \sqrt{\frac{4\kappa}{T_m}} \int_{T_j}^{T_j+T_m} dt \tilde{a}_-^{in}(t) \frac{[1 - e^{-(\kappa + \kappa_L)(T_j + T_m - t)}]}{(\kappa + \kappa_L)}. \end{aligned} \quad (65)$$

Using Eq. (63) in Eq. (62), we find that the correlation matrix V^{out} can be decomposed into the sum of three contributions,

$$V^{out} = \alpha(T_m)^2 V + V^{in} + V^{mix}, \quad (66)$$

where V^{in} is the contribution due to the input noise term $n^{in}(T_j, T_m)$, V^{mix} is the contribution due to the correlation between the intracavity fields at the end of the pulses $\tilde{a}(T_j)$ and the input noises, and V is the correlation ma-

trix for the quadratures of the intracavity fields $X(T_j) = (\tilde{a}(T_j) + \tilde{a}^\dagger(T_j))/\sqrt{2}$, $P(T_j) = -i(\tilde{a}(T_j) - \tilde{a}^\dagger(T_j))/\sqrt{2}$. Its elements have the form

$$V_{kl} = \frac{\langle \xi_k \xi_l + \xi_l \xi_k \rangle}{2}, \quad (67)$$

where we have defined the four-dimensional vector $\xi^T = (X(T_1), P(T_1), X(T_2), P(T_2))$, and are reported in App. C. Using the correlation functions of the input

noises $\tilde{a}^{in}(t)$ and $\tilde{a}_-^{in}(t)$ one finds that V^{in} is proportional to the 4×4 identity matrix

$$V^{in} = \frac{1}{2} [1 - \alpha(T_m)^2] \delta_{ij}, \quad (68)$$

while V^{mix} has only four nonzero terms, which are all identical, $V_{13}^{mix} = V_{31}^{mix} = V_{24}^{mix} = V_{42}^{mix} = \mathcal{V}^{mix}$, with

$$\mathcal{V}^{mix} = \alpha(T_m) \sqrt{\frac{\kappa}{2T_m}} \frac{e^{-(\kappa+\kappa_L)(T-T_1)} g_{-2}(T_2-T)}{\kappa+\kappa_L} \left\{ e^{-(\kappa+\kappa_L)T_m} - 1 \right\}. \quad (69)$$

Equation (69) shows that the contributions due to correlations between intracavity fields at the end of the pulse and input noise are zero as soon as we choose the optimal transfer condition $g_{-2}(T_2-T) = 0$ of Eq. (57) (They are in any case negligible when $(\kappa+\kappa_L)(T-T_1) \gg 1$).

Let us now consider what is the optimal integration time T_m , such that $V^{out} \approx V$, i.e. the correlation matrix at the cavity output reproduces the correlation matrix between the intracavity fields. From Eqs. (66) and (68) we see that T_m must be chosen such that the quantity $\alpha(T_m)$ is as close as possible to unity. In this case, most of the intracavity field is detected at the cavity output at the end of the pulse, and at the same time the contribution of the input noise is negligible. From Eq. (64) one gets that $\alpha(T_m) \leq \alpha_{max}$, where $\alpha_{max} \simeq 0.9/\sqrt{1+\kappa_L/\kappa} < 1$, and it is achieved for $T_m^0 \simeq 1.25/(\kappa+\kappa_L)$.

In order to establish the conditions under which the two output pulses are entangled we consider the logarithmic negativity $E_{\mathcal{N}}$, a quantity which has been already proposed as a measure of entanglement [41]. In the continuous variable case $E_{\mathcal{N}}$ can be defined as [42]

$$E_{\mathcal{N}} = \max[0, -\ln 2\eta^-], \quad (70)$$

where

$$\eta^- \equiv 2^{-1/2} \left[\Sigma(V^{out}) - [\Sigma(V^{out})^2 - 4 \det V^{out}]^{1/2} \right]^{1/2}, \quad (71)$$

with $\Sigma(V^{out}) \equiv \det A + \det B - 2 \det C$, and we have used the 2×2 block form of the correlation matrix

$$V^{out} \equiv \begin{pmatrix} A & C \\ C^T & B \end{pmatrix}. \quad (72)$$

Therefore, a Gaussian state is entangled if and only if $\eta^- < 1/2$. This is equivalent to Simon's necessary and sufficient entanglement criterion for Gaussian states of a non-positive partial transpose [43], which can be written as $4 \det V < \Sigma - 1/4$.

We finally comment on our choice to quantify the entanglement in terms of the logarithmic negativity instead

of EPR variances [32]. The latter would seem a natural choice, but in fact they provide an unambiguous characterization of entanglement *only* for simple examples of CV two-mode entangled states, such as the two-mode squeezed state. Any reasonable entanglement measure has to be invariant under local transformations of the quadratures of each mode separately. In our system, however, the common definition of EPR correlations [42, 43] reads

$$\xi_{EPR} = \frac{1}{2} [\Delta(X^{out}(T_1, T_m) - X^{out}(T_2, T_m))^2 + \Delta(P^{out}(T_1, T_m) + P^{out}(T_2, T_m))^2],$$

with $\Delta(A)^2$ the variance of A , and depends upon the chosen set of quadratures, i.e. it does not possess such invariance. The light pulses at the cavity output are in a two-mode squeezed state only in the ideal limit when the noise contributions to the dynamics are negligible, and when the ion's motional state created by the first pulse is perfectly transferred to the second pulse. Under realistic conditions the state of the two pulses is rather different from a two-mode squeezed state; therefore using EPR variances would give an ambiguous quantification of the generated entanglement. Nonetheless, there is a connection between squeezing and the measure of entanglement provided by the logarithmic negativity. To be more specific, a simple and direct quantitative connection between EPR variances and $E_{\mathcal{N}}$ can be found in the case of *symmetric* bipartite states, i.e., states which are invariant under exchange of the two modes (the two pulses in our case) [42]. In such a case, the quantity $2\eta^- = \exp(-E_{\mathcal{N}})$ gives the largest amount of EPR correlations, that is, the minimum achievable value of ξ_{EPR} which can be attained in the CV bipartite state by means of local operations, i.e. by considering all possible linear combinations of the quadratures of each pulse.

IV. RESULTS

We now analyze the basic requirements and the efficiency of this scheme using parameters accessible in present experiments with atoms in resonators. Our considerations follow and extend the corresponding discussion in [31]. For comparison, we will discuss along with some realistic sets of parameters an idealised case where the cavity decay rate is set to a very small value, and the noise terms are suppressed.

The atom's internal degrees of freedom need to provide an optical dipole transition which couples to both the laser and the cavity mode. A suitable example would be an $F=0 \leftrightarrow F'=1$ closed atomic transition with the quantization axis \vec{B} along the cavity axis, and \vec{B} , \vec{k}_L , and laser polarization \vec{E}_L mutually orthogonal. Ideal candidates would then be alkali-earth-metal atoms or alkali-earth-metal-like ions, but other geometries can be found which allow for the realization of this scheme using also alkali atoms or alkali-like ions. We consider an alkali-earth atom in the geometrical configuration $\theta_L = 0$, $\theta_c = \pi/2$, and $\phi_c = 0$. This means that the trap center coincides with an antinode of the cavity mode, and that the motion takes place along the direction of the laser beam and orthogonally to the cavity axis, such that there is no mechanical effect of the cavity field on the motion. This assumption is not strictly necessary but it is made here in order to simplify the discussion.

In order to favor motional Raman transitions over resonant scattering, we assume a value of the atom-field detuning Δ which exceeds the values of the coupling strengths Ω and $g_c\sqrt{n}$, (n is the average number of cavity photons), and of the atomic transition linewidth γ . Taking a typical value of the linewidth of an optical dipole transition, $\gamma = 2\pi \times 5$ MHz, we choose $|\Delta| = 2\pi \times 120$ MHz, $\Omega = 2\pi \times 10$ MHz and $g_c = 2\pi \times 1$ MHz, which are accessible values for state-of-the-art experiments with trapped atoms or ions in resonators [15, 19, 44].

We also consider the motion to be restricted to the Lamb-Dicke regime, with a Lamb-Dicke parameter $\eta = 0.1$. This leads to $|\chi_1|, |\chi_2| \simeq 2\pi \times 8$ kHz for the coupling constants, while the loss rates associated with the various scattering processes are $\kappa_L \sim \kappa_{\pm j}^b \simeq 2\pi \times 0.2$ kHz. The trap frequency can be set to $\nu \simeq 2\pi \times 1$ MHz, which is typical in ion trap experiments [45]. The heating rate of the vibrational motion may be estimated as $\kappa_h \simeq 2\pi \times 20$ Hz [46, 47].

The value of the cavity decay rate κ must warrant the coherent creation of correlations during the pulses ($\kappa T_{1,2} \ll 1$), as well as spectral resolution of the sidebands ($\kappa \ll \nu$). In the examples we discuss we assume values that range from $\kappa \simeq 2\pi \times 20$ kHz, which is experimentally accessible [44, 48], down to $2\pi \times 1$ kHz, which is more difficult to reach with present-day technology, but serves as an idealised case for comparison.

Given the parameters, finally the laser pulse durations T_1 and $T_2 - T$, as well as their separation T must be adjusted in order to (i) create significant entanglement be-

tween the first pulse and the motion, and (ii) efficiently realise the quantum state transfer between the motion and the second pulses. At the same time the motion, which acts as intermediate quantum memory, needs to remain coherent during laser excitation and cavity output.

We first focus on the dependence upon the duration of the second pulse, $T_2 - T$. The optimization of the state transfer from the center-of-mass motion to the cavity mode discussed in Sec. IIB.3 yielded the condition of Eq. (57), $T_2 - T = \delta T_2^{opt}$. Therefore we expect the entanglement to be maximum around this condition. This is confirmed by Fig. 3, where the logarithmic negativity is plotted versus the normalized duration of the second pulse, $(T_2 - T)/\delta T_2^{opt}$ at various values of the cavity decay rate. The duration of the first pulse has been fixed at $T_1 = 40 \mu\text{sec} \simeq 2/|\chi_1|^{-1}$, while the time interval between the two pulses has been chosen to be related to the cavity decay time according to $T - T_1 = 2/(\kappa + \kappa_L)$; the other parameter values are those discussed above. It is evident that the entanglement between the pulses is optimized when the duration of the second pulse satisfies Eq. (57).

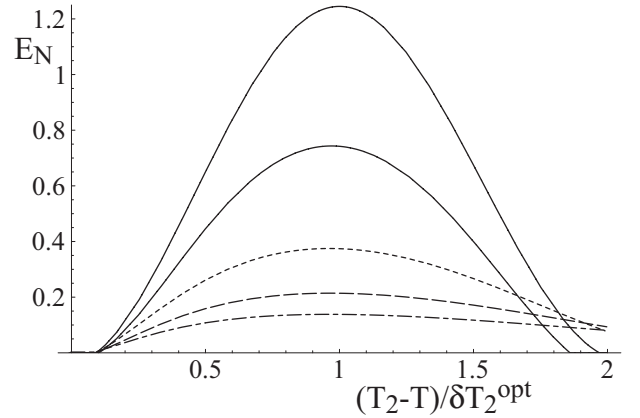


FIG. 3: Logarithmic negativity E_N versus normalized duration of the second pulse $(T_2 - T)/\delta T_2^{opt}$ (see Eq. (57)) at four different values of the cavity decay rate. From bottom to top, $\kappa = 2\pi \times (16, 11, 6.4, 0.8, 0.8)$ kHz; the top solid curve is plotted for comparison and corresponds to the smallest value of κ with all other noise terms set to zero. The other parameter values are $(|\Delta|, \gamma, \Omega, g_c, \nu) = 2\pi \times (120, 5, 10, 1, 1)$ MHz and $\eta = 0.1$, yielding $(|\chi_1|, |\chi_2|, \kappa_L, \kappa_{\pm j}^b) = 2\pi \times (8.5, 8.5, 0.18, 0.18)$ kHz; the heating rate is $\kappa_h = 2\pi \times 20$ Hz. The duration of the first pulse is fixed at $T_1 = 40 \mu\text{s} \sim 2/|\chi_1|^{-1}$, while for each curve, the time interval between the two pulses is related to the cavity decay time according to $T - T_1 = 2/(\kappa + \kappa_L) = (20, 28, 49, 327, 400) \mu\text{s}$ (bottom to top).

The dependence of the logarithmic negativity E_N upon the time separation $T - T_1$ between the two pulses is shown in Fig. 4. Parameter values are the same as in

Fig. 3 except that we have fixed the duration of the second pulse at the optimal value $T_2 - T = \delta T_2^{opt}$ given by Eq. (57). Entanglement (i.e. E_N) decays essentially linearly, and notably its lifetime is independent from the cavity decay rate κ . In fact, E_N always vanishes when $T - T_1 \simeq \kappa_h^{-1}$, i.e. the two pulses are entangled provided that their separation is not larger than the vibrational heating time κ_h^{-1} . This is not surprising because the vibrational motion acts as the continuous-variable quantum memory mediating the entanglement, and thus the heating time limits the achievable coherent storage time.

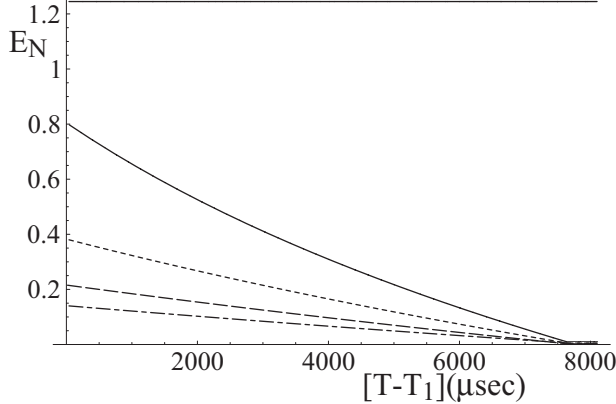


FIG. 4: Logarithmic negativity E_N versus the time separation between the two pulses $T - T_1$ at the same values of the cavity decay rate κ as in Fig. 3. The other parameter values are also the same as in Fig. 3 except that the duration of the second pulse has been fixed at the optimal value $T_2 - T = \delta T_2^{opt} = (19, 22, 24, 29, 29) \mu s$ (bottom to top).

Finally, the dependence of the logarithmic negativity upon the duration of the first pulse T_1 is shown in Fig. 5. The other two timing parameters are, for each curve, $T_2 - T = \delta T_2^{opt}$ as in Fig. 4, and $T - T_1 = 2/(\kappa + \kappa_L)$ as in Fig. 3. The rest of the parameters have the same values as before. E_N is always increasing and then tends to saturate at a value that, as expected, is larger for smaller cavity decay rates. In presence of noise one finds an empirical expression for the asymptotic logarithmic negativity given by $E_N^{asym} \simeq \ln[4|\chi_1|/\kappa]/4$. This behavior can be intuitively explained by the fact that the first laser pulse entangles the cavity mode and the vibrational motion like in a parametric amplifier, and this continuous variable entanglement increases for increasing T_1 . Cavity losses, however, limit the entanglement generation and are ultimately responsible for the saturation of the entanglement at larger T_1 .

From Fig. 5 it can be seen that choosing a large T_1 , in the saturation regime, has two advantages: i) entanglement is maximized; ii) the scheme is insensitive to

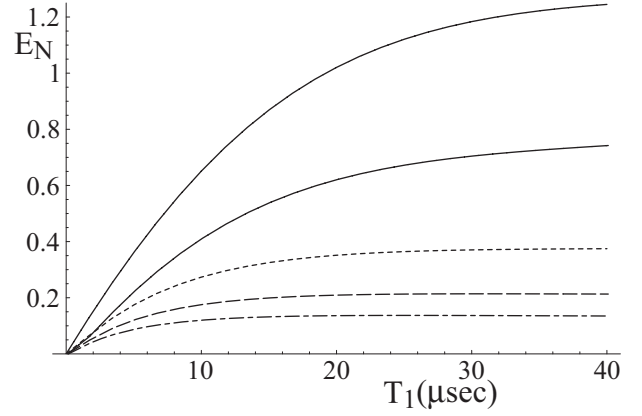


FIG. 5: Logarithmic negativity E_N versus duration of the first laser pulse T_1 , for the same values of κ as in the previous figures. The time interval between the two pulses and the duration of the second pulse are set for each curve according to $T - T_1 = 2/(\kappa + \kappa_L)$ and $T_2 - T = \delta T_2^{opt}$. The other parameter values are the same as before.

fluctuations of T_1 . It must be kept in mind, however, that we are considering the entanglement between two output light pulses which are counted for a time interval $T_m^0 = 1.25/(\kappa + \kappa_L)$ starting only when each exciting laser pulse has finished (see Sec. III). This means that for large values of T_1 the detection of the two entangled pulses is more difficult, especially when the cavity decay rate is large. In these latter cases, the number of photons leaving the cavity *during* the first excitation pulse is larger than the average number of photons in the two detected output pulses. In the saturation regime $T_1 = 40 \mu s$, the average number of photons per entangled pulse is $\bar{n}(T_1) = \langle \tilde{a}^\dagger(T_1) \tilde{a}(T_1) \rangle = (12.38, 3.65, 1.55, 0.76)$ for $\kappa = 2\pi \times (0.8, 6.4, 11, 16)$ kHz, where we have set $T_m^0 = 1.25/(\kappa + \kappa_L)$, while the other parameters are as in the figures.

V. CONCLUSIONS

To conclude, we have characterized the quantum correlations of two temporally separated entangled light pulses, emitted from a single atom inside an optical cavity, in the set-up first proposed in [30, 31]. By means of a quantum noise analysis we have quantified the amount of entanglement one can extract from this system for experimentally accessible parameter regimes, and we have shown that the quantum motion of a single trapped particle is an efficient quantum medium which creates and mediates entanglement on demand between subsequent radiation pulses.

This scheme offers promising perspectives for atom-photon interfaces and for devising new cryptographic schemes exploiting time-correlated pulses and continuous alphabets, thus extending those based on time-bin entangled photon pairs [34]. The scheme may also be

easily generalised to the generation of two pulses of different frequencies, or even at vastly different wavelengths, by varying appropriately the frequency or wavelength of the second excitation pulse.

An interesting outlook is to study the scalability of the scheme when the number of atoms composing the quantum medium is increased in a controlled way, hence characterizing which resources the collective excitations of the medium may offer for creating entangled light.

VI. ACKNOWLEDGEMENTS

The authors acknowledge discussions with Stefano Mancini. This work was partly supported by the European Commission ("CONQUEST", MRTN-CT-2003-505089; "EMALI", MRTN-CT-2006-035369; "SCALA", Contract No. 015714), by the Spanish Ministerio de Educación y Ciencia ("QOIT", Consolider Ingenio 2010 CSD2006-00019; "LACSMY", FIS2004-05830; "QLIQS", FIS2005-08257; "QNLP", FIS2007-66944; Ramon-y-Cajal program), and by the Italian Ministero dell'Università e Ricerca (PRIN-2005024254).

APPENDIX A: MECHANICAL EFFECTS IN THE LANGEVIN FORCE

We derive the Langevin force considering the mechanical effects of the spontaneously emitted photon on the atom. At this purpose, we consider a simple model, constituted by a dipole of frequency ω_0 at position x and Hamiltonian of the center of mass H_{CM} ,

$$H_{at} = \hbar\omega_0|e\rangle\langle e| + H_{CM}$$

The dipole is coupled to the modes of the e.m.-field at frequency ω_s and Hamiltonian

$$H_{emf} = \sum_s \hbar\omega_s a_s^\dagger a_s,$$

with interaction Hamiltonian

$$H_{int} = \hbar \sum_s g_s e^{ik_s x} \sigma^\dagger a_s + \text{H.c.}$$

where g_s is the vacuum Rabi frequency. The formal solution of the Heisenberg equation for a_s gives

$$a_s(t) = e^{-i\omega_s t} a_s(0) - ig_s \int_0^t d\tau e^{-i\omega_s \tau} e^{-ik_s x(t-\tau)} \sigma(t-\tau) \quad (A1)$$

We substitute this result into the Heisenberg equation for σ , and obtain

$$\begin{aligned} \dot{\sigma} = & -i\omega_0 \sigma + i\sigma_z \sum_s g_s e^{ik_s x} e^{-i\omega_s t} a_s(0) \\ & + \sigma_z \sum_s g_s^2 \int_0^t e^{ik_s [x(t)-x(t-\tau)]} e^{-i\omega_s \tau} \sigma(t-\tau) \end{aligned} \quad (A2)$$

We make now the Markov approximation, assuming that the characteristic frequencies of the center of mass motion are much smaller than the optical frequencies of the e.m.-field, which couple quasi-resonantly with the dipole. Hence, in the integral we approximate $x(t-\tau) \approx x(t)$. Taking $\sigma(t-\tau) \approx e^{i\omega_0 \tau} \sigma(t)$, we obtain

$$\begin{aligned} \dot{\sigma} = & -i\omega_0 \sigma + \sigma_z i \sum_s g_s e^{ik_s x} e^{-i\omega_s t} a_s(0) \\ & - \sigma(t) \sum_s g_s^2 \int_0^\infty e^{i(\omega_0 - \omega_s)\tau} d\tau \end{aligned} \quad (A3)$$

The integral gives a real term, the linewidth $\gamma = 2\pi \sum_s g_s^2 \delta(\omega_0 - \omega_s)$, and an imaginary part, the Cauchy principal value shifting the transition frequency. Including this shift in the value of ω_0 we obtain

$$\dot{\sigma} = -i\omega_0 \sigma - \frac{\gamma}{2} \sigma + i\sigma_z F_0(t) \quad (A4)$$

with the noise source

$$F_0(t) = \sum_s g_s e^{ik_s x} e^{-i\omega_s t} a_s(0) \quad (A5)$$

such that $\langle F_0(t) F_0(t')^\dagger \rangle = \gamma \delta(t-t')$. Let us now investigate the form of $F_0(t)$ when the center of mass motion is a harmonic oscillator, $H_{CM} = H_{mec}$ given by Eq. (3). Applying the Lamb-Dicke expansion, $F_0(t)$ takes the form

$$\begin{aligned} F_0(t) = & \sum_s g_s e^{-i\omega_s t} a_s(0) \\ & \times \left(1 - \frac{\eta^2}{2} \cos^2 \theta_s (2b^\dagger b + 1) + i\eta \cos \theta_s (b^\dagger + b) \right) \end{aligned} \quad (A6)$$

with $k_s x = \eta \cos \theta_s (b^\dagger + b)$, where θ_s is the angle between the wave vector of the emitted photon and the axis of the motion. Taking the continuous limit of the sum, we separate the integrals over the modulus and the polar angle, and over the azimuthal angle $\theta = \theta_s$, obtaining $F_0(t) \approx F(t)$, with

$$\begin{aligned} F(t) = & \sqrt{\gamma} \int d\cos\theta \sqrt{\mathcal{N}(\cos\theta)} f_\theta^{in}(t) \\ & \times \left(1 - \frac{\eta^2}{2} \cos^2 \theta (2b^\dagger b + 1) + i\eta \cos \theta (b^\dagger + b) \right), \end{aligned} \quad (A7)$$

where $\mathcal{N}(\cos\theta)$ is the dipole pattern of emission, $\int d\cos\theta \mathcal{N}(\cos\theta) = 1$ and $f_\theta^{in}(t)$ are the angle-dependent Langevin forces,

$$\langle f_\theta^{in}(t) f_{\theta'}^{in\dagger}(t') \rangle = \delta(\theta - \theta') \delta(t - t'), \quad (A8)$$

and which have zero mean value.

APPENDIX B: EFFECTIVE QUANTUM LANGEVIN EQUATIONS

First laser pulse. Starting from Eqs. (23)-(24), which are defined in the reference frame of the laser, we

move to a frame rotating at the effective vibrational angular frequency $\nu' \simeq \nu$, and we neglect all the terms oscillating at ν' or larger. This approximation is justified in the regime we consider, where we assume that the Stokes and anti-Stokes sidebands are spectrally resolved.

The operators in this reference frame are connected to the ones in the reference frame of the laser by the transformation $\tilde{a}^\dagger(t) = e^{i\nu't} a^\dagger(t)$, $\tilde{b}(t) = e^{i\nu't} b(t)$, and their equations of motion have the explicit form

$$\begin{aligned} \dot{\tilde{a}}^\dagger(t) = & i(\nu' - \delta_1) \tilde{a}^\dagger(t) - \kappa \tilde{a}^\dagger(t) + \sqrt{2\kappa} \tilde{a}^{in}(t)^\dagger - \int_0^t ds e^{-(\frac{\gamma}{2} + i\Delta_1)s} [B^\dagger(t-s) + F^\dagger(t-s)] e^{i\nu't} \\ & \times \left[g_c \cos \phi_c \left(1 - \frac{\eta^2}{2} \cos^2 \theta_c (2\tilde{b}^\dagger \tilde{b} + 1) \right) - \eta g_c \sin \phi_c \cos \theta_c \left(\tilde{b}(t) e^{-i\nu't} + \tilde{b}^\dagger(t) e^{i\nu't} \right) \right], \end{aligned} \quad (B1)$$

$$\begin{aligned} \dot{\tilde{b}}(t) = & i(\nu' - \nu) \tilde{b}(t) - \kappa_b \tilde{b}(t) + \sqrt{2\kappa_b} \tilde{b}^{in}(t) + \int_0^t ds e^{-(\frac{\gamma}{2} - i\Delta_1)s} [B(t-s) + F(t-s)] e^{i\nu't} \\ & \times \left[i\eta \Omega_1^* \cos \theta_L + \eta g_c^* \sin \phi_c \cos \theta_c \tilde{a}^\dagger(t) e^{-i\nu't} + \eta^2 \tilde{b}(t) e^{-i\nu't} \left(\Omega_1^* \cos^2 \theta_L + g_c^* \cos \phi_c \cos^2 \theta_c \tilde{a}^\dagger(t) e^{-i\nu't} \right) \right. \\ & \left. + i\eta \sqrt{\gamma} \langle f_\theta^{in\dagger}(t) \cos \theta \rangle_\theta + \eta^2 \sqrt{\gamma} \tilde{b}(t) e^{-i\nu't} \langle f_\theta^{in\dagger}(t) \cos^2 \theta \rangle_\theta \right] - \int_0^t ds e^{-(\frac{\gamma}{2} + i\Delta_1)s} [B^\dagger(t-s) + F^\dagger(t-s)] e^{i\nu't} \\ & \times \left[-i\eta \Omega_1 \cos \theta_L + \eta g_c \sin \phi_c \cos \theta_c \tilde{a}(t) e^{i\nu't} + \eta^2 \tilde{b}(t) e^{-i\nu't} \left(\Omega_1 \cos^2 \theta_L + g_c \cos \phi_c \cos^2 \theta_c \tilde{a}(t) e^{i\nu't} \right) \right. \\ & \left. - i\eta \sqrt{\gamma} \langle f_\theta^{in}(t) \cos \theta \rangle_\theta + \eta^2 \sqrt{\gamma} \tilde{b}(t) e^{-i\nu't} \langle f_\theta^{in}(t) \cos^2 \theta \rangle_\theta \right], \end{aligned} \quad (B2)$$

where $\langle \dots \rangle_\theta$ in the equation for $\dot{\tilde{b}}(t)$ denotes the average over the azimuthal angle θ with weight given by the dipole pattern of emission $\mathcal{N}(\cos \theta)$, and we have introduced the noise operators $\tilde{a}^{in}(t) \equiv e^{-i\nu't} a^{in}(t)$ and $\tilde{b}^{in}(t) \equiv e^{i\nu't} b^{in}(t)$, which are still delta-correlated. We use the explicit expression for $B(t-s)$, thereby neglecting the terms oscillating at ν' or faster, and perform the

time integrals by making the Markovian approximation $\exp\{-(\gamma/2 \pm i\Delta_1 + im\nu')s\} \approx \delta(s)/(\gamma/2 \pm i\Delta_1 + im\nu')$, for $m = -1, 0, 1$.

After long, but straightforward calculations we get the final, effective HLE at leading order in the Lamb-Dicke parameter, which read

$$\dot{\tilde{a}}^\dagger(t) = i(\nu' - \delta_1 + \delta') \tilde{a}^\dagger(t) + \chi_1^* \tilde{b}(t) - (\kappa + \kappa_L) \tilde{a}^\dagger(t) + \sqrt{2\kappa} \tilde{a}^{in}(t)^\dagger + \sqrt{2\kappa_L} \tilde{a}_-^{in}(t)^\dagger + F_a, \quad (B3)$$

$$\begin{aligned} \dot{\tilde{b}}(t) = & i(\nu' - \nu - \delta_1^b) \tilde{b}(t) + \bar{\chi}_1 \tilde{a}^\dagger(t) - (\kappa_b + \kappa_{+1}^b - \kappa_{-1}^b) \tilde{b}(t) \\ & + \sqrt{2\kappa_b} \tilde{b}^{in}(t) + \sqrt{2\kappa_{+1}^b} \tilde{a}_+^{in}(t) - \sqrt{2\kappa_{-1}^b} \tilde{a}_-^{in}(t)^\dagger + F_b. \end{aligned} \quad (B4)$$

Here, the coefficients

$$\chi_1 = \eta \Omega_1 g_c^* \cos \phi_c \left(\frac{\cos \theta_L}{\Delta_1 - \nu' + i\gamma/2} + \frac{i \tan \phi_c \cos \theta_c}{\Delta_1 + i\gamma/2} \right), \quad (B5)$$

$$\bar{\chi}_1 = \eta \Omega_1 g_c^* \cos \phi_c \left(\frac{\cos \theta_L}{\Delta_1 - \nu' - i\gamma/2} + \frac{i \tan \phi_c \cos \theta_c}{\Delta_1 + i\gamma/2} \right), \quad (B6)$$

correspond to the Raman processes in which laser photons are scattered into the cavity mode with a change in the center-of-mass excitation. Since we assume $\gamma \ll |\Delta_1|$

(and also $\nu \ll |\Delta_1|$), we shall take $\bar{\chi}_1 = \chi_1$, and approximate χ_1 with Eq. (30). The noise operators $\tilde{a}_\pm^{in}(t)$ are defined in Eqs. (31)-(32), while the rates κ_L , $\kappa_{\pm 1}^b$ in Eqs. (33)-(35). The noise scaling factors $\bar{\kappa}_{\pm 1}^b$ of Eq. (36) are generally given by

$$\begin{aligned} \bar{\kappa}_{+1}^b &= i\eta \sqrt{\frac{\gamma}{2}} \left(\frac{\Omega_1 \cos \theta_L}{\gamma/2 - i(\Delta_1 + \nu')} - \frac{\Omega_1^* \langle \cos \theta \rangle_\theta}{\gamma/2 + i\Delta_1} \right) \\ \bar{\kappa}_{-1}^b &= -i\eta \sqrt{\frac{\gamma}{2}} \left(\frac{\Omega_1 \cos \theta_L}{\gamma/2 + i(\Delta_1 - \nu')} + \frac{\Omega_1^* \langle \cos \theta \rangle_\theta}{\gamma/2 - i\Delta_1} \right), \end{aligned}$$

but they reduce to the expression of Eq. (36) because the average over the dipole pattern gives $\langle \cos \theta \rangle_\theta = 0$.

The operators F_a and F_b in Eqs. (B3)-(B4) represent non-linear noise terms, associated with incoherent scattering processes. They give rise to a.c.-Stark shift and losses, whose effect is in general detrimental for the effectiveness of the two-mode squeezing processes, and are of the form $F_a \sim \eta^2 g^2 \tilde{a} \tilde{b}^\dagger \tilde{b} / (\Delta + i\gamma/2)$, $F_b \sim \eta^2 g^2 \tilde{a}^\dagger \tilde{a} \tilde{b} / (\Delta + i\gamma/2)$, hermitian conjugates, and corresponding input noise operators. These terms can be neglected in comparison with the laser induced Raman scattering processes whenever the inequality $\Omega_1 \cos \theta_L \gg g_c \sqrt{n} \cos \theta_c$ is satisfied (n is the average number of cavity photons), which is a condition on the parameters and on the geometry of the setup. We will assume this regime, and these terms will be neglected during the laser pulses. In this regime, the frequency shifts of the cavity mode and of the vibrational motion read

$$\delta' = \frac{(\Delta_1 - \nu') |g_c|^2 \cos^2 \phi_c}{\gamma^2/4 + (\Delta_1 - \nu')^2} \quad (\text{B7})$$

$$\delta_1^b = 2\eta^2 |\Omega_1|^2 \cos^2 \theta_L \Delta_1 \quad (\text{B8})$$

$$\left(\frac{\gamma^2/4 + \Delta_1^2 - \nu'^2}{(\gamma^2/4 + \Delta_1^2 - \nu'^2)^2 + \nu'^2 \gamma^2} - \frac{1}{\Delta_1^2 + \gamma^2/4} \right).$$

These shifts must be taken into account when tuning the frequency of the first laser pulse. In particular, since the dynamics we seek relies on the resonant two-photon processes, where a laser photon is absorbed and a the cavity photon and a vibrational phonon are emitted, hence the cavity mode frequency must be exactly at resonance with the Stokes sideband of the driving laser, i.e.,

$$\omega_{L1} = \omega_c + \delta' + \nu + \delta\nu. \quad (\text{B9})$$

Here, $\delta\nu$ can be extracted from Eq. (B8) when $|\delta\nu| \ll \nu$, which is satisfied provided that $\eta |\Omega_1| \ll |\Delta_1|$ and $\eta |\Omega_1/\Delta_1| \ll \nu$, and reads

$$\delta\nu \approx \frac{2\Delta_1 \eta^2 |\Omega_1|^2 \cos^2 \theta_L (\gamma^2/4 + \Delta_1^2 - \nu^2)}{(\gamma^2/4 + \Delta_1^2 - \nu^2)^2 + \nu^2 \gamma^2}$$

$$- 2\eta^2 |\Omega_1|^2 \cos^2 \theta_L \frac{\Delta_1}{\Delta_1^2 + \gamma^2/4}. \quad (\text{B10})$$

Consequently,

$$\nu' = \nu + \delta\nu \quad (\text{B11})$$

determines the effective frequency of the Stokes sideband.

We notice that the resonant condition (B9), giving the relation $\omega_{L1} - \nu' = \omega_c + \delta'$, gives us a simple relation between the observables in laboratory frame and the "tilded" observables, which are connected by the relations

$$a_{\text{lab}}(t) = e^{-i(\omega_c + \delta')t} \tilde{a}(t) \quad (\text{B12})$$

$$b_{\text{lab}}(t) = e^{-i\nu' t} \tilde{b}(t). \quad (\text{B13})$$

Second laser pulse. The main difference with the treatment of the dynamics during the first pulse is that the second pulse is set to a different resonance condition, e.g.

$$\omega_{L2} = \omega_c - \nu'', \quad (\text{B14})$$

where $\nu'' \simeq \nu$ and the difference accounts for the a.c.-Stark shifts induced by the second laser pulse on cavity and motion frequency. When condition (B14) is fulfilled, the cavity mode is resonant with the anti-Stokes motional sideband of the laser light, with angular frequency $\omega_{L2} + \nu''$. Spectral resolution of this resonance is warranted when $\nu T_2 \gg 1$ and $\nu \gg \kappa, \kappa_b$.

In the reference frame rotating at the frequency of the cavity mode, the HLE read

$$\dot{\tilde{a}}(t) = i(\nu'' + \delta_2) \tilde{a}(t) - \kappa \tilde{a}(t) + \sqrt{2\kappa} \tilde{a}^{\text{in}}(t) + \int_0^t ds e^{-(\frac{\gamma}{2} - i\Delta_2)s} [B(t-s) + F(t-s)] e^{i\nu'' t} \quad (\text{B15})$$

$$\times \left[-g_c^* \cos \phi_c \left(1 - \frac{\eta^2}{2} \cos^2 \theta_c (2\tilde{b}^\dagger \tilde{b} + 1) \right) + \eta g_c^* \sin \phi_c \cos \theta_c \left(\tilde{b}(t) e^{-i\nu'' t} + \tilde{b}^\dagger(t) e^{i\nu'' t} \right) \right],$$

$$\dot{\tilde{b}}(t) = i(\nu'' - \nu) \tilde{b}(t) - \kappa_b \tilde{b}(t) + \sqrt{2\kappa_b} \tilde{b}^{\text{in}}(t) + \int_0^t ds e^{-(\frac{\gamma}{2} - i\Delta_2)s} [B(t-s) + F(t-s)] e^{i\nu'' t} \quad (\text{B16})$$

$$\times \left[i\eta \Omega_2^* \cos \theta_L + \eta g_c^* \sin \phi_c \cos \theta_c \tilde{a}^\dagger(t) e^{i\nu'' t} + \eta^2 \tilde{b}(t) e^{-i\nu'' t} \left(\Omega_2^* \cos^2 \theta_L + g_c^* \cos \phi_c \cos^2 \theta_c \tilde{a}^\dagger(t) e^{i\nu'' t} \right) \right. \\ \left. + i\eta \sqrt{\gamma} \langle f_\theta^{\text{in}\dagger}(t) \cos \theta \rangle_\theta + \eta^2 \sqrt{\gamma} \tilde{b}(t) e^{-i\nu'' t} \langle f_\theta^{\text{in}\dagger}(t) \cos^2 \theta \rangle_\theta \right] - \int_0^t ds e^{-(\frac{\gamma}{2} + i\Delta_2)s} [B^\dagger(t-s) + F^\dagger(t-s)] e^{i\nu'' t} \\ \times \left[-i\eta \Omega_2 \cos \theta_L + \eta g_c \sin \phi_c \cos \theta_c \tilde{a}(t) e^{-i\nu'' t} + \eta^2 \tilde{b}(t) e^{-i\nu'' t} \left(\Omega_2 \cos^2 \theta_L + g_c \cos \phi_c \cos^2 \theta_c \tilde{a}(t) e^{-i\nu'' t} \right) \right. \\ \left. - i\eta \sqrt{\gamma} \langle f_\theta^{\text{in}}(t) \cos \theta \rangle_\theta + \eta^2 \sqrt{\gamma} \tilde{b}(t) e^{-i\nu'' t} \langle f_\theta^{\text{in}}(t) \cos^2 \theta \rangle_\theta \right]$$

where the noise operators $\tilde{a}^{in}(t)$ and $\tilde{b}^{in}(t)$ are the same as in Eqs. (B1)-(B2). Following the procedure outlined

before, we finally get the coupled HLE

$$\dot{\tilde{a}}(t) = i(\nu' + \delta_2 - \delta')\tilde{a}(t) + \chi_2\tilde{b}(t) - (\kappa + \kappa_L)\tilde{a}(t) + \sqrt{2\kappa}\tilde{a}^{in}(t) + \sqrt{2\kappa_L^*}\tilde{a}_+^{in}(t) + F_a, \quad (\text{B17})$$

$$\dot{\tilde{b}}(t) = i(\nu' - \nu - \delta_2^b)\tilde{b}(t) - \bar{\chi}_2^*\tilde{a}(t) - (\kappa_b + \kappa_{+2}^b - \kappa_{-2}^b)\tilde{b}(t) + \sqrt{2\kappa_b}\tilde{b}^{in}(t) + \sqrt{2\kappa_{+2}^b}\tilde{a}_+^{in}(t) - \sqrt{2\kappa_{-2}^b}\tilde{a}_-^{in}(t)^\dagger + F_b \quad (\text{B18})$$

Let us now define the coefficients appearing in these equations. The quantities κ_L and δ' are given by Eq. (33) and (B7), respectively. In fact, together with $\bar{\kappa}_L$, they do not depend upon the properties of the driving laser; moreover the two noise operators $\tilde{a}_-^{in}(t)$ and $\tilde{a}_+^{in}(t)$ are given by Eqs. (31) and (32). The nonlinear terms F_a and F_b are the same as in Eqs. (B3)-(B4), and are negligible as we take $\Omega_2 \cos \theta_L \gg g_c \cos \theta_c$. The coupling constants associated with the Raman scattering processes are

$$\chi_2 = \eta\Omega_2 g_c^* \cos \phi_c \left(\frac{\cos \theta_L}{\Delta_2 + \nu' + i\gamma/2} + \frac{i \tan \phi_c \cos \theta_c}{\Delta_2 + i\gamma/2} \right), \quad (\text{B19})$$

$$\bar{\chi}_2 = \eta\Omega_2 g_c^* \cos \phi_c \left(\frac{\cos \theta_L}{\Delta_2 + \nu' - i\gamma/2} + \frac{i \tan \phi_c \cos \theta_c}{\Delta_2 + i\gamma/2} \right). \quad (\text{B20})$$

As we consider the limit $\gamma \ll |\Delta_2|$ we shall take $\bar{\chi}_2 = \chi_2$ from now on. The incoherent emission or absorption of a vibrational quantum scales with the rates

$$\kappa_{\pm 2}^b = \frac{\gamma}{2} \frac{\eta^2 \cos^2 \theta_L \Omega_2^2}{\gamma^2/4 + (\Delta_2 \pm \nu')^2}, \quad (\text{B21})$$

and in the limit $|\Delta_2| \gg \gamma, \nu$ the rates scaling the input noise read

$$\bar{\kappa}_{-2}^b = -i\eta\sqrt{\frac{\gamma}{2}} \frac{\Omega_2 \cos \theta_L}{\gamma/2 + i(\Delta_2 - \nu'')} \\ \bar{\kappa}_{+2}^b = i\eta\sqrt{\frac{\gamma}{2}} \frac{\Omega_2^* \cos \theta_L}{\gamma/2 - i(\Delta_2 + \nu'')}.$$

Finally, the frequency shift of the vibrational motion reads

$$\delta_2^b = \frac{2\Delta_2\eta^2|\Omega_2|^2 \cos^2 \theta_L (\gamma^2/4 + \Delta_2^2 - \nu'^2)}{(\gamma^2/4 + \Delta_2^2 - \nu'^2)^2 + \nu'^2\gamma^2} \quad (\text{B22}) \\ - \eta^2|\Omega_2|^2 \cos^2 \theta_L \frac{2\Delta_2}{\Delta_2^2 + \gamma^2/4}$$

For $|\Delta_2| \gg \gamma, \eta|\Omega_2/\Delta_2| \ll \nu$, we find with good approximation

$$\delta_2^b \approx \frac{2\Delta_2\eta^2|\Omega_2|^2 \cos^2 \theta_L (\gamma^2/4 + \Delta_2^2 - \nu'^2)}{(\gamma^2/4 + \Delta_2^2 - \nu'^2)^2 + \nu'^2\gamma^2} \\ - \eta^2|\Omega_2|^2 \cos^2 \theta_L \frac{2\Delta_2}{\Delta_2^2 + \gamma^2/4}, \quad (\text{B23})$$

determining, together with Eq. (B7), the resonance condition for the central frequency of the laser pulse,

$$\delta_2 = \omega_{L2} - \omega_c = \delta' - \nu - \delta_2^b. \quad (\text{B24})$$

For $|\Delta_2| \gg \nu$, choosing $\Omega_2 = \Omega_1$, then $\delta_2^b \approx \delta_1^b$, $\nu'' = \nu'$ and the processes leading to absorption of a phonon and emission of a cavity photon are resonantly enhanced by choosing the frequency of the second laser pulse at $\omega_{L2} = \omega_c - \nu'$. We consider this regime, as it simplifies substantially the calculations. When it is not fulfilled, one must consider an accumulated phase, which gives simply a total phase shift and hence modifies the quadratures exhibiting entanglement.

APPENDIX C: CALCULATION OF THE ELEMENTS OF THE CORRELATION MATRIX

We derive here the elements of the intracavity correlation matrix V of Eq. (67), using that the cavity modes and the vibrational motion are initially in the vacuum state, and the fact that input noise is uncorrelated with the cavity mode operators at former times. The elements read

$$V_{12} = 0 \quad (\text{C1})$$

$$V_{11} = V_{22} = \langle \tilde{a}^\dagger(T_1)\tilde{a}(T_1) \rangle + 1/2$$

$$V_{33} = \langle \tilde{a}^\dagger(T_2)\tilde{a}(T_2) \rangle + \text{Re} \{ \langle \tilde{a}^\dagger(T_2)^2 \rangle \} + 1/2$$

$$V_{44} = \langle \tilde{a}^\dagger(T_2)\tilde{a}(T_2) \rangle - \text{Re} \{ \langle \tilde{a}^\dagger(T_2)^2 \rangle \} + 1/2$$

$$V_{34} = -\text{Im} \{ \langle \tilde{a}^\dagger(T_2)\tilde{a}^\dagger(T_2) \rangle \}$$

$$V_{13} = [\langle \tilde{a}(T_1)\tilde{a}(T_2) \rangle + \langle \tilde{a}(T_1)\tilde{a}^\dagger(T_2) \rangle \\ + \langle \tilde{a}^\dagger(T_1)\tilde{a}(T_2) \rangle + \langle \tilde{a}^\dagger(T_1)\tilde{a}^\dagger(T_2) \rangle + c.c.] / 4$$

$$V_{24} = -[\langle \tilde{a}(T_1)\tilde{a}(T_2) \rangle - \langle \tilde{a}(T_1)\tilde{a}^\dagger(T_2) \rangle \\ - \langle \tilde{a}^\dagger(T_1)\tilde{a}(T_2) \rangle + \langle \tilde{a}^\dagger(T_1)\tilde{a}^\dagger(T_2) \rangle + c.c.] / 4$$

$$V_{14} = -i[\langle \tilde{a}(T_1)\tilde{a}(T_2) \rangle - \langle \tilde{a}(T_1)\tilde{a}^\dagger(T_2) \rangle \\ + \langle \tilde{a}^\dagger(T_1)\tilde{a}(T_2) \rangle - \langle \tilde{a}^\dagger(T_1)\tilde{a}^\dagger(T_2) \rangle - c.c.] / 4$$

$$V_{23} = -i[\langle \tilde{a}(T_1)\tilde{a}(T_2) \rangle + \langle \tilde{a}(T_1)\tilde{a}^\dagger(T_2) \rangle \\ - \langle \tilde{a}^\dagger(T_1)\tilde{a}(T_2) \rangle - \langle \tilde{a}^\dagger(T_1)\tilde{a}^\dagger(T_2) \rangle - c.c.] / 4$$

Using Eqs. (37), (46) and (50) we obtain

$$\langle \tilde{a}^\dagger(T_1) \tilde{a}(T_1) \rangle = |\chi_1|^2 \left(|f_1(T_1)|^2 + (\kappa_h + 2|\bar{\kappa}_{+1}^b|^2) \int_0^{T_1} ds |f_1(s)|^2 \right) \quad (C2)$$

$$\begin{aligned} \langle \tilde{a}^\dagger(T_2) \tilde{a}(T_2) \rangle &= |g_{-2}(T_2 - T)|^2 e^{-2(\kappa + \kappa_L)(T - T_1)} \langle \tilde{a}^\dagger(T_1) \tilde{a}(T_1) \rangle + |\chi_2|^2 |f_2(T_2 - T)|^2 e^{-2\kappa_b(T - T_1)} \langle \tilde{b}^\dagger(T_1) \tilde{b}(T_1) \rangle \\ &\quad + |\chi_2|^2 (\kappa_h + 2|\bar{\kappa}_{-2}^b|^2) \int_0^{T_2 - T} |f_2(s)|^2 + \frac{\kappa_h}{2\kappa_b} |\chi_2|^2 |f_2(T_2 - T)|^2 \left(1 - e^{-2\kappa_b(T - T_1)} \right) \end{aligned} \quad (C3)$$

$$\langle \tilde{a}(T_1) \tilde{a}(T_2) \rangle = \chi_2 f_2(T_2 - T) e^{(i\delta_1^b - \kappa_b)(T - T_1)} \langle \tilde{a}(T_1) \tilde{b}(T_1) \rangle \quad (C4)$$

$$\langle \tilde{a}^\dagger(T_1) \tilde{a}^\dagger(T_2) \rangle = \langle \tilde{a}(T_1) \tilde{a}(T_2) \rangle^* \quad (C5)$$

$$\langle \tilde{a}^\dagger(T_2) \tilde{a}^\dagger(T_1) \rangle = 2\chi_2^* f_2(T_2 - T) g_{-2}(T_2 - T) e^{-(i\delta_1^b + \kappa_b + \kappa_L + \kappa)(T - T_1)} \langle \tilde{a}^\dagger(T_1) \tilde{b}^\dagger(T_1) \rangle \quad (C6)$$

$$\langle \tilde{a}(T_1) \tilde{a}^\dagger(T_2) \rangle = g_{-2}(T_2 - T) e^{-(\kappa_L + \kappa)(T - T_1)} \langle \tilde{a}(T_1) \tilde{a}^\dagger(T_1) \rangle \quad (C7)$$

$$\langle \tilde{a}^\dagger(T_1) \tilde{a}(T_2) \rangle = \langle \tilde{a}(T_1) \tilde{a}^\dagger(T_2) \rangle^* \quad (C8)$$

where we have used $\kappa_h = \kappa_b(2\bar{N} + 1)$, and that $\kappa_h \gg \kappa_b$. In deriving these relation we also used that $\langle \tilde{a}^\dagger(T_1) \tilde{b}(T_1) \rangle = \langle \tilde{a}(T_1) \tilde{b}^\dagger(T_1) \rangle = 0$. In order to fully de-

termine the above relations as a function of the initial conditions, we need

$$\langle \tilde{b}^\dagger(T_1) \tilde{b}(T_1) \rangle = |\chi_1|^2 |f_1(T_1)|^2 + \kappa_h \int_0^{T_1} ds |g_{+1}(s)|^2 + 2\kappa |\chi_1|^2 \int_0^{T_1} ds |f_1(s)|^2 \quad (C9)$$

$$\begin{aligned} &+ 2 \int_0^{T_1} ds |\bar{\kappa}_{-1}^b g_{+1}(s) - \chi_1 \bar{\kappa}_L f_1(s)|^2 \\ \langle \tilde{a}(T_1) \tilde{b}(T_1) \rangle &= g_{-1}(T_1) \chi_1 f_1(T_1) + \chi_1 (\kappa_h - 2\kappa_b) \int_0^{T_1} ds f_1(s) g_{+1}(s) \\ &+ 2 \int_0^{T_1} ds (\bar{\kappa}_{-1}^* \chi_1 f_1(s) - \bar{\kappa}_L^* g_{-1}(s)) (\bar{\kappa}_{-1}^b g_{+1}(s) - \bar{\kappa}_L \chi_1 f_1(s)) + 2\kappa \chi_1 \int_0^{T_1} g_{-1}(s) f_1(s) \end{aligned} \quad (C10)$$

In deriving these expressions we used that the HLE conserve the commutation relations. This is not fulfilled

for long times, when the perturbative expansion loses validity.

-
- [1] A. Kuzmich, W.P. Bowen, A.D. Boozer, A. Boca, C.W. Chou, L.-M. Duan, and H.J. Kimble, *Nature* **423**, 731 (2003).
 - [2] V. Josse, A. Dantan, L. Vernac, A. Bramati, M. Pinard, E. Giacobino, *Phys. Rev. Lett.* **91**, 103601 (2003); V. Josse, A. Dantan, A. Bramati, M. Pinard, E. Giacobino, *Phys. Rev. Lett.* **92**, 123601 (2004).
 - [3] C. H. van der Wal, M. D. Eisaman, A. André, R. L. Walsworth, D. F. Phillips, A. S. Zibrov, M. D. Lukin, *Science* **301**, 196 (2003).
 - [4] M. D. Lukin, *Rev. Mod. Phys.* **75**, 457 (2003).
 - [5] B. Julsgaard, J. Sherson, J. I. Cirac, J. Fiurasek, and E. S. Polzik, *Nature* **432**, 482 (2004).
 - [6] C. W. Chou, H. de Riedmatten, D. Felinto, S. V. Polyakov, S. J. van Enk, and H. J. Kimble, *Nature* **438**, 828 (2005).
 - [7] J.F. Sherson, *et al.*, *Nature* **443**, 557 (2006).
 - [8] J. M. Raimond, M. Brune, S. Haroche, *Rev. Mod. Phys.* **73**, 565 (2001).
 - [9] H. Walther, B.T.H. Varcoe, B.-G. Englert, T. Becker, *Rep. Prog. Phys.* **69**, 1325 (2006).
 - [10] K. An, J. J. Childs, R. R. Dasari, and M. S. Feld, *Phys. Rev. Lett.* **73**, 3375 (1994).
 - [11] J. McKeever, A. Boca, A. D. Boozer, J. R. Buck and H. J. Kimble, *Nature* **425**, 268 (2003).
 - [12] C. J. Hood, T. W. Lynn, A. C. Doherty, A. S. Parkins, and H. J. Kimble, *Science* **287**, 1457 (2000);
 - [13] P. W. H. Pinkse, T. Fischer, P. Maunz, and G. Rempe,

- Nature **404**, 365 (2000).
- [14] P. Bushev, A. Wilson, J. Eschner, C. Raab, F. Schmidt-Kaler, C. Becher, and R. Blatt, Phys. Rev. Lett. **92**, 223602 (2004).
 - [15] A. B. Mundt, A. Kreuter, C. Becher, D. Leibfried, J. Eschner, F. Schmidt-Kaler, R. Blatt, Phys. Rev. Lett. **89**, 103001 (2002).
 - [16] G. R. Guthöhrlein, M. Keller, K. Hayasaka, W. Lange, H. Walther, Nature **414**, 49 (2001).
 - [17] A. Kuhn, M. Hennrich, and G. Rempe, Phys. Rev. Lett. **89**, 067901 (2002); T. Legero, T. Wilk, M. Hennrich, G. Rempe, and A. Kuhn, Phys. Rev. Lett. **93**, 070503 (2004).
 - [18] J. McKeever, A. Boca, A. D. Boozer, R. Miller, J. R. Buck, A. Kuzmich and H. J. Kimble, Science **303**, 1992 (2004).
 - [19] M. Keller, B. Lange, K. Hayasaka, W. Lange, and H. Walther, Nature **431**, 1075 (2004).
 - [20] B. Blinov, D. L. Moehring, L.-M. Duan, and C. Monroe, Nature (London) **428**, 153 (2004).
 - [21] J. Volz, M. Weber, D. Schlenk, W. Rosenfeld, J. Vrana, K. Saucke, C. Kurtsiefer, H. Weinfurter, Phys. Rev. Lett. **96**, 030404 (2006).
 - [22] D.L. Moehring, P. Maunz, S. Olmschenk, K.C. Younge, D. N. Matsukevich, L.-M. Duan, and C. Monroe, Nature **449**, 68 (2007).
 - [23] A. D. Boozer, A. Boca, R. Miller, T. E. Northup, and H. J. Kimble, Phys. Rev. Lett. **98**, 193601 (2007).
 - [24] J. I. Cirac, P. Zoller, H. J. Kimble, and H. Mabuchi, Phys. Rev. Lett. **78**, 3221 (1997).
 - [25] B. Kraus and J. I. Cirac, Phys. Rev. Lett. **92**, 013602 (2004).
 - [26] S. L. Braunstein and P. van Loock, Rev. Mod. Phys. **77**, 513 (2005).
 - [27] H. Zeng and F. Lin, Phys. Rev. A **50**, R3589 (1994).
 - [28] A. S. Parkins and H. J. Kimble, J. Opt. B: Quantum Semiclass. Opt. **1**, 496 (1999).
 - [29] A. Peng and A. S. Parkins, Phys. Rev. A **65**, 062323 (2002).
 - [30] G. Morigi, J. Eschner, S. Mancini, and D. Vitali, Phys. Rev. Lett. **96**, 023601 (2006).
 - [31] G. Morigi, J. Eschner, S. Mancini, and D. Vitali, Phys. Rev. A **73**, 033822 (2006).
 - [32] M.D. Reid, Phys. Rev. A **40**, 913 (1989).
 - [33] F. Grosshans, G. Van Assche, J. Wenger, R. Brouri, N.J. Cerf and Ph. Grangier, Nature (London) **421**, 238 (2003).
 - [34] See N. Gisin, G. Ribordy, W. Tittel and H. Zbinden, Rev. Mod. Phys. **74**, 145 (2002) and references therein.
 - [35] Note that Eqs. (7) and (9) are at first order in the Lamb-Dicke parameter, nevertheless we have included also the term $\eta^2(2b^\dagger b + 1)$, which belongs to the second-order expansion. This term gives rise to a.c.-Stark shifts induced by the field, which should be systematically taken into account when one considers transition rates between vibrational states (which are at second order in η). See for instance [38, 45].
 - [36] D. F. Walls and G. J. Milburn, *Quantum Optics*, (Springer, Berlin, 1994).
 - [37] S. Schneider and G.J. Milburn, Phys. Rev. A **59**, 3766 (1998); S. Mancini, D. Vitali, and P. Tombesi, Phys. Rev. A **61**, 053404 (2000).
 - [38] D. Vitali, G. Morigi, and J. Eschner, Phys. Rev. A **74**, 053814 (2006).
 - [39] The rates in Eq. (35) can be put in relation with the cooling and heating rates of the rate equations of cooling, see S. Stenholm, Rev. Mod. Phys. **58**, 699 (1986). In particular, for $\Delta < 0$ then $\kappa_{+1}^b > \kappa_{-1}^b$ and in this case, in absence of the cavity coupling, the motion would be cooled.
 - [40] S.J. van Enk and C.A. Fuchs, Phys. Rev. Lett. **88**, 027902 (2002)
 - [41] G. Vidal and R. F. Werner, Phys. Rev. A **65**, 032314 (2002).
 - [42] G. Adesso *et al.*, Phys. Rev. A **70**, 022318 (2004).
 - [43] R. Simon, Phys. Rev. Lett. **84**, 2726 (2000).
 - [44] C. Maurer, C. Becher, C. Russo, J. Eschner, and R. Blatt, New J. Phys. **6**, 94 (2004).
 - [45] J. Eschner, G. Morigi, F. Schmidt-Kaler, and R. Blatt, J. Opt. Soc. Am. B **20**, 1003 (2003).
 - [46] D. M. Lucas, B. C. Keitch, J. P. Home, G. Imreh, M. J. McDonnell, D. N. Stacey, D. J. Szwer, and A. M. Steane, preprint, arXiv:0710.4421 (2007).
 - [47] J. Labaziewicz, Y. Ge, P. Antohi, D. Leibbrandt, K. R. Brown, I. L. Chuang, "Suppression of Heating Rates in Cryogenic Surface-Electrode Ion Traps", preprint arXiv:0706.3763 (2007).
 - [48] J. A. Sauer, K. M. Fortier, M. S. Chang, C. D. Hamley, and M. S. Chapman, Phys. Rev. A **69**, 051804(R) (2004).